

Density Functional Theory with Optimized Effective Potential: An Application to Hollow Atoms in the Bulk of Metallic Materials

Xiao-Min Tong^{a*} (全曉民), Daiji Kato^a (加藤太治), Tsutomu Watanabe^b (渡部力), Hiroshi Shimizu^a (清水宏), Chikashi Yamada^{a,c} (山田千櫻) and Shunsuke Ohtani^{a,c} (大谷俊介)

^a*Cold Trapped Ions Project, ICORP, JST, Axis 3F, 1-40-2 Fuda Chofu, Tokyo 182-0024, Japan*

^b*Division of Natural Sciences, International Christian University, Ohsawa, Mitaka-shi, Tokyo 118-8585, Japan*

^c*University of Electro-Communication, Chofu, Tokyo 182-0021, Japan*

The local spin-density functional theory with an optimized effective potential and self-interaction correction is used to study the energy structure of hollow atoms or ions in the bulk of metallic materials. The energy structure of conduction electrons in the bulk of metallic material is treated by the jellium model. Based on this method, we have studied the emitted x-ray spectra of Ar^{q+} hollow atoms and ions in the bulk of Ag as well as in the vacuum. By comparing the energy spectra of Ar^{q+} hollow atoms or ions in the vacuum and in the bulk of Ag, we can illustrate the conduction electron screening effect. Our calculated x-ray spectra of Ar^{q+} hollow atoms or ions in the bulk of Ag is in reasonable agreement with the experiment.

I. INTRODUCTION

The interaction of highly charged ions (HCI) with surfaces is a subject of increasing interest.¹⁻³ Basically, three steps are involved in the interaction of HCI with surfaces: (1) the formation of hollow atoms or ions above surfaces; (2) the decay of hollow atoms or ions at or below surfaces and (3) total neutralization of hollow atoms or ions in the bulk of materials.¹ The formation of hollow atoms or ions is strongly related to the HCI's impact velocity, incident angle and other dynamic parameters.⁴ In the final neutralization step, hollow atoms or ions emit Auger electrons^{5,6} or x-rays.⁷⁻⁹ The emitted x-ray can provide static information of hollow atoms or ions in the bulk of materials from the energy position and the dynamic information from the spectral intensity. Usually, the Hartree-Fock method is used to study the energy structure of hollow atoms or ions in a vacuum,^{10,11} which can not provide the detailed information of hollow atoms or ions in the bulk of materials. The conduction electron screening effect was first studied by Zaremba et al.¹² by use of the density functional theory. Recently, Arnau et al.¹³ have used the local density functional theory to study the energy structure of hollow atoms and ions in the bulk of metallic materials. The advantage of this method is that the total energy of the N-electron system is a function of the total electron density. Similar to the traditional local density functional theory,¹⁴ such a method contains a spurious self-interaction energy, which

should be removed in the exact calculation. To remove the self-interaction energy, we use the local spin density approximation with an optimized effective potential and self-interaction correction (LSDA/OEP-SIC) method.¹⁵⁻¹⁷ Such a method has been successfully applied to study the atomic energy structure both in the non-relativistic¹⁶ and relativistic¹⁸ cases. Different from atoms or ions in a vacuum, hollow atoms or ions in the bulk of metallic materials interact with free electrons in the conduction band as well. The conduction electron is treated by the jellium model at present. The advantages of our method are: 1) we use local spin-density approximation, which allows us to study the spin polarized hollow atoms or ions in the bulk of metallic materials; 2) we use the optimized effective potential with self-interaction correction for bound electrons, which can completely remove the self-interaction energy for bound electrons.

Based on this method, we have studied the energy structure of N^{q+} ions in the bulk of Al.¹⁹ Now, we will study the energy structure of Ar^{q+} ions in the bulk of Ag, the emitted x-ray energy from $K^1 L^y M^x$ to $K^2 L^{y-1} M^x$ configurations and so on. We will give a brief description of our theoretical method in Sec. II and present our results and discussion in Sec. III.

II. THEORETICAL METHOD

The energy structure of conduction electrons in a metal

lic material can be studied by the jellium model.²⁰ In the jellium model, the discrete ion cores are replaced by a homogeneous positive background with the charge density equal to the conduction electron density due to the neutralization requirement. For a given electron density ρ , an effective radial $r_s = (3/(4\pi\rho))^{1/3}$ is defined and the conduction electrons are filled up to the Fermi energy $\varepsilon_F = \frac{1}{2r_s^2}(9\pi/4)^{2/3}$. Based on the density functional theory with the optimized effective potential and self-interaction correction,¹⁶ the total energy of a hollow atom or ion in the bulk of metallic materials (the jellium model) can be expressed as:

$$\begin{aligned} E[\rho] = & T_s[\rho] + E_{xc}[\rho_\uparrow, \rho_\downarrow] + V_{ext}[\rho] + J_A[\rho] + E^{SIC}[\rho_b] \\ & - T_s[\rho_o] - E_{xc}[\rho_{o\uparrow}, \rho_{o\downarrow}] - V_{ext}[\rho_o], \end{aligned} \quad (1)$$

with

$$\begin{aligned} V_{ext}[\rho] &= -\int \frac{Z}{r} \rho(\mathbf{r}) d\mathbf{r}, \\ J_A[\rho] &= \frac{1}{2} \int \frac{\rho(\mathbf{r}')\rho(\mathbf{r})}{|\mathbf{r}'-\mathbf{r}|} d\mathbf{r}' d\mathbf{r} - \int \frac{\rho(\mathbf{r}')\rho_o}{|\mathbf{r}'-\mathbf{r}|} d\mathbf{r}' d\mathbf{r} \\ &+ \frac{1}{2} \int \frac{\rho_o \rho_o}{|\mathbf{r}'-\mathbf{r}|} d\mathbf{r}' d\mathbf{r}, \\ \rho(\mathbf{r}) &= \sum_{\sigma} (\rho_{i\sigma}(\mathbf{r}) + \rho_{o\sigma} + \delta\rho_{c\sigma}(\mathbf{r})) \\ &= \rho_b(\mathbf{r}) + \rho_o + \delta\rho_c(\mathbf{r}). \end{aligned}$$

Here, $T_s[\rho]$ is the non-interacting electron kinetic energy, $E_{xc}[\rho]$, the exchange-correlation energy, $E^{SIC}[\rho_b]$, the self-interaction correction for bound electrons and σ , the spin index (spin-up and spin-down states). ρ_o is the background conduction electron density, ρ_b , the bound electron density and $\delta\rho_c$, the conduction electron density changes due to the introduction of the hollow atom or ion. The background energy without the hollow atom or ion is subtracted in Eq. (1). The electron wave functions can be obtained by solving the following Schrödinger equation as

$$\left[-\frac{\nabla^2}{2} + V_{\sigma}^{OEP}(\mathbf{r}) \right] \Psi_{i\sigma}(\mathbf{r}) = \varepsilon_{i\sigma} \Psi_{i\sigma}(\mathbf{r}), \quad (2)$$

with

$$\begin{aligned} V_{\sigma}^{OEP}(\mathbf{r}) &= \int \frac{\rho_b(\mathbf{r}') + \delta\rho_c(\mathbf{r}')}{|\mathbf{r}-\mathbf{r}'|} d\mathbf{r}' + \frac{\delta E_{xc}[\rho_\uparrow, \rho_\downarrow]}{\delta\rho_o} \\ &+ V_{\sigma}^{SIC}(\mathbf{r}) - \frac{Z}{r} + V_{const}, \\ \rho_{b\sigma}(\mathbf{r}) &= \sum_b \Psi_{i\sigma}^*(\mathbf{r}) \Psi_{i\sigma}(\mathbf{r}), \\ \delta\rho_{c\sigma}(\mathbf{r}) &= \sum_l \int_0^{k_f} \Psi_{i\sigma}^*(r, k) \Psi_{i\sigma}(r, k) dk - \rho_{o\sigma}. \end{aligned} \quad (3)$$

Note that $r\Psi_{i\sigma}(r, k) \rightarrow \sqrt{2/\pi} \sin(kr - l\pi/2 + 2\pi\delta_l)$ when $r \rightarrow \infty$, here δ_l is the phase shift and k_f , the electron momentum at the Fermi energy.

The bottom of the Fermi energy is chosen as zero of the energy. Eqs. (2) and (3) can be solved self-consistently. Since both the bond and continuum states are involved in Eq. (2), we use a non-equal space radial grid in the inner region and an equal space radial grid in the outer region. The advantage of the grid structure is that we can describe both the bound and continuum states accurately with limited computational effort. With the converged effective potential in Eq. (3), we can obtain the electron spin-density distribution, total energy and phase shift for each partial wave and so on.

From the theoretical point of view, the improvements of the present method¹⁹ over the previous one¹³ are: (1) we use the local spin-density functional approximation, which allows us to study the spin-polarized hollow atoms or ions in the bulk of metallic materials; (2) we include explicitly self-interaction correction for bound electrons, which can give a better orbital energy and total energy.^{16,18,19}

III. RESULTS AND DISCUSSION

Based on the LSDA/OEP-SIC method, we have calculated the energy structure of Ar^{q+} ions in the bulk of Ag. In the calculation, the conduction electrons are treated by the jellium model with $r_s = 1.60$. Although the energy structure of Ar^{q+} hollow atoms or ions is labeled by $K^n L^m M^x$ followed by the convention in Ref. 13, it still has many configurations within each configuration. We listed all the L^y configurations used in the calculation in Table 1. In practice, we calculated the total energy for all possible spin combinations within each L^y configuration listed in Table 1. For the M^x configurations, we fill the M-shell from $3s$ first and then $3p$ sequentially for simplicity. With such configurations, we calculated the total energies of transition upper and lower states (with $1s$

Table 1. The Configurations Used in the Calculation

| L^1 | L^2 | L^3 | L^4 |
|-------------|-----------------------|--------------------------------------|--------------------------------------|
| $2p^1$ | $2s^1 2p^1$ $2p^2$ | $2s^2 2p^1$ $2s^1 2p^2$ $2p^3$ | $2s^2 2p^2$ $2s^1 2p^3$ $2p^4$ |
| L^5 | L^6 | L^7 | L^8 |
| $2s^2 2p^3$ | $2s^2 2p^4$ | $2s^2 2p^5$ | |
| $2s^1 2p^4$ | $2s^1 2p^5$ | $2s^1 2p^6$ | $2s^2 2p^6$ |
| $2s^1 2p^5$ | $2p^6$ | | |

vacancy filled by a $2p$ electron in the upper state), emitting x-ray energy, screening effect and phase shift. We will discuss each in detail.

A. Total energies of Ar^{q+} ions in the bulk of Ag and in the vacuum

We have performed the total energy calculations for Ar^{q+} ions in the vacuum and in the bulk of Ag by LSDA/OEP-SIC method. To compare the two calculations of Ar^{q+} ions in the vacuum and in the bulk of Ag, we can illustrate the screening effect of conduction electrons. Fig. 1 shows the total energies of Ar^{q+} ions in the vacuum as well as in the bulk of Ag. Generally speaking, the total energy decreases as the number of bound electrons increases. For Ar^{q+} ions in the bulk of Ag, the changes of the total energy with the number of electrons in the M-shell are very smooth. For Ar^{q+} ions in the vacuum, such changes are much rapid than that of Ar^{q+} ions in the bulk of Ag. Such observation can be understood as: when we add one more electron into the system in the vacuum, the total energy will decrease rapidly. For Ar^{q+} ions in the bulk of Ag, due to the neutralization requirement, if we add one more electron, the less effect nucleus charge will attract less conduction electrons, the total energy changes a little due to the fact the net charge change around the nucleus is almost zero.

Also we can see that adding one more electron into the

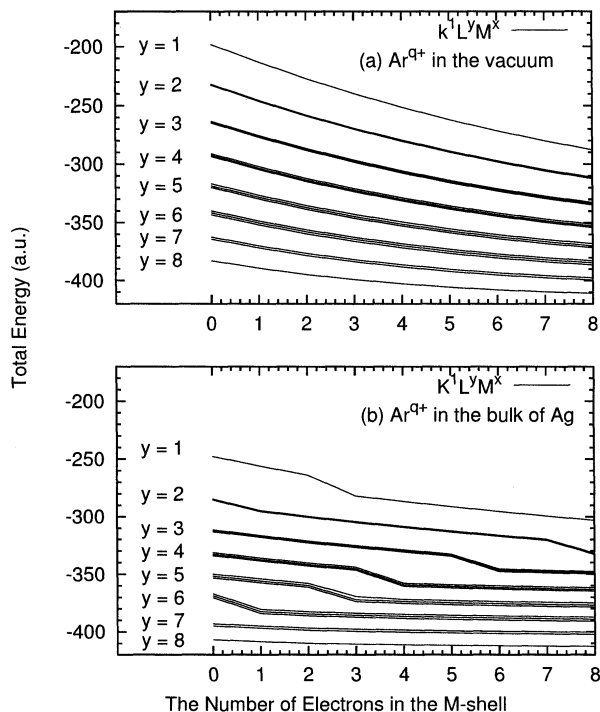


Fig. 1. The total energies of Ar^{q+} ions in (a) the vacuum and (b) the bulk of Ag.

L-shell will release more energies than adding one more electron into the M-shell as shown in Fig. 1. The energy difference for a given hollow atom or ion in the vacuum and the bulk of material will be released when the hollow atom or ion approaches to the surface.

The total energy of Ar^{q+} ions in the bulk of Ag shows a dramatic change for some given configurations as shown in Fig. 1. This is due to the fact that the short-range potential changes dramatically when one electron is added or removed from that configuration. Detailed discussion will be presented in the discussion of phase shifts.

B. X-ray spectrum of Ar^{q+} ions in the bulk of Ag

With the calculated total energy, we can obtain the x-ray transition energy as

$$\hbar\nu = E_{total}[K^1L^yM^x] - E_{total}[K^2L^{y-1}M^x] \quad (4)$$

for a given configuration. The calculated energies are shown in Fig. 2(a) by the solid vertical line. To clearly see the shell structure, we offset one for each band (with the same number of electrons in the L-shell). We also show the correspondence value of Ar^{q+} ions in the vacuum by the dashed vertical line.

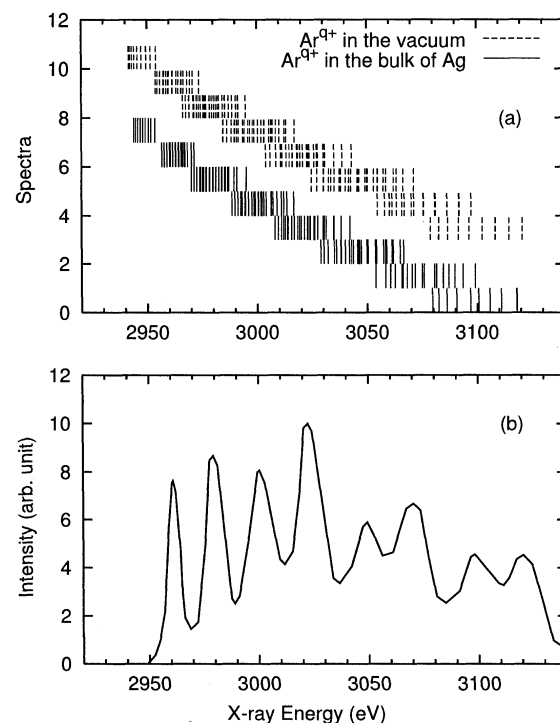


Fig. 2. (a) The calculated x-ray energies of Ar^{q+} ions in the bulk of Ag (solid line) and in the vacuum (dashed line), and (b) the experimental x-ray spectra.⁷

Note that the dashed line is offset by 4. For the spectra of Ar^{q+} ions in the vacuum, the energy levels are overlapped for different bands due to the filling of the M-shell. Thus, we can roughly claim that spectra in some energy region corresponds to the contribution for a given configuration, but not definitely. The experimental spectra can be expressed as

$$I(E) \propto \sum_i P(i) R_r(i) e^{-(E-E_r(i))^2/2\tau^2}, \quad (5)$$

with $P(i)$, the percentage of a given hollow atom or ion formed in the bulk of materials, $R_r(i)$, radiative decay rate of the hollow atom or ion, $E_r(i)$, transition energy of radiative decay and τ , energy resolution in the experiments. Here we use the Gaussian line profile. In Eq. (5), to reproduce the experiment spectrum, we need static information ($R_r(i)$, $E_r(i)$) and dynamic information $P(i)$ and experimental energy resolution τ . In turn, if we know the experimental spectrum, we can abstract the dynamic information based on the calculated static properties ($R_r(i)$, $E_r(i)$).

For Ar^{q+} ions in the bulk of Ag, the spectra for given L^q fold is narrower than that in the vacuum, and the spectra for L^8 is clearly separated from other folds. This is due to the conduction electron screening effect, the same as we discussed above. The experimental spectra⁷ are also shown in Fig. 2(b). By comparing with our calculated spectra, we can roughly assign each peak. The detailed assignment is still impossible since we do not know the dynamical information involved in the experiment. To compare with the experiment spectra, we need the percentage of each hollow atom or ion for a given configuration, which is strongly dependent on the experiment conditions, namely, the HCl's velocity, incident angle and so on. But our structure calculation can still provide some physical information and can help the experimenter to identify the spectra.

C. Density changes of conduction electrons

Based on the jellium model, the conduction electrons are homogeneous distributed over the whole bulk. With the introducing of Ar^{q+} ions into the material, the homogeneous electron gas will be perturbed and the density change is defined as

$$\delta\rho_c(r) = \rho_c(r) - \rho_o. \quad (6)$$

Since induced potential by Ar^{q+} ions is of a spherical symmetry, the density change is also of a spherical symmetry; here, we only show the radial density changes. Fig. 3 shows the conduction electron density changes with the perturbation of Ar^{q+} ions for $K^1L^1M^0$, $K^1L^1M^8$, $K^1L^8M^0$ and $K^1L^8M^8$ configura-

tions, respectively, and the correspondence transition lower states. The four cases represent the situations of Ar^{q+} ions with almost empty L and M-shell electrons and full filled L and M-shell electrons. With the less bound electrons ($K^1L^1M^0$), more conduction electrons are attracted to the nucleus, which provide a screening field for the outer electrons. With most bound electrons ($K^1L^8M^8$), a few conduction electrons are attracted to the nucleus. For $K^1L^1M^8$, due to the full-filled M-shell electrons, the free electron is difficult to penetrate into the inner region. The total bound electron of $K^1L^8M^0$ is almost the same as $K^1L^1M^8$, but with inner-shell full-filled, the perturbed electrons are concentrated relatively close to the nucleus. It is also true for the transition lower states, as shown in Fig. 3(b). Since the conduction electron density changes strongly relate to the phase shift, we will discuss the phase shift in detail.

D. Phase shifts

Fig. 4 shows the calculated phase shifts for the s , p , and f partial waves in four electron configurations. Based on the Levinson theorem,²¹ we conclude that 3 bound states (1s, 2s, 3s) exist for the s partial wave with the full filled L shell configurations $K^1L^8M^0$, $K^1L^8M^8$, and one more s bound state appears for $K^1L^1M^8$ and two more s bound states appear for $K^1L^1M^0$. In the vacuum, the number of bound states is infinite,

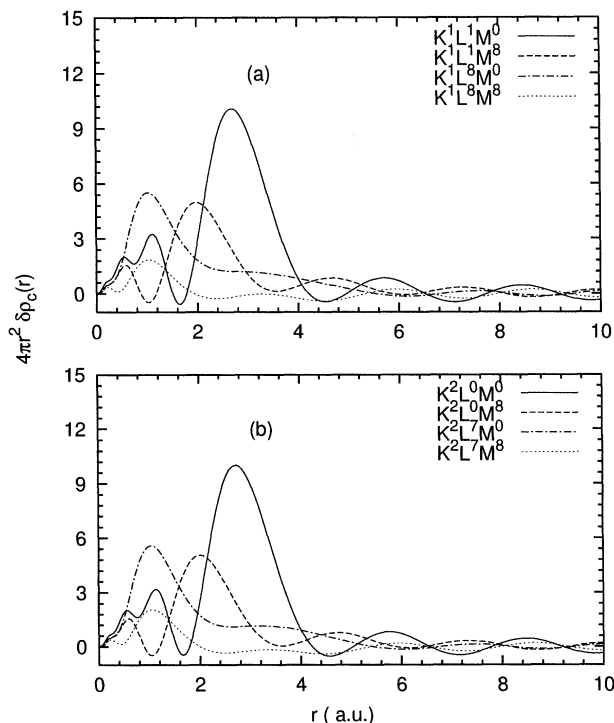


Fig. 3. Conduction electron density changes for the transition (a) initial and (b) final states.

which is different from the case in the bulk of metallic materials. Such things also appear in the *p*, *d* and *f* partial waves as shown in Fig. 4. Apart from the *p*-partial wave in the $K^1L^1M^0$ configuration, all the phase shifts of the *s* and *p* partial waves decrease monotonically as the energy increases. The phase shifts of the *d* and *f* partial waves increase as the energy increases. For $K^1L^1M^0$ configuration, the phase shift of the *p* partial wave increases first, then decreases as the energy increases. From the Friedel sum rule,²²

$$N_c = Z - N_b = \sum_{lq} (2l+1)(\delta_{lq}(\epsilon_F) - \delta_{lq}(0)), \quad (7)$$

with *Z* as the atomic number, *N_b*, the number of bound electrons in the hollow atom or ion, we can see that the screening electron comes from the *d* and *f* partial waves. Note that we have checked the total number of electrons within r_{max} sphere, which is in good agreement with *Z*. The calculated phase shifts are also very important for studying the stopping power of the low energy HCl moving in the bulk of metallic materials.²³⁻²⁵

To summarize, we have studied the energy structure of

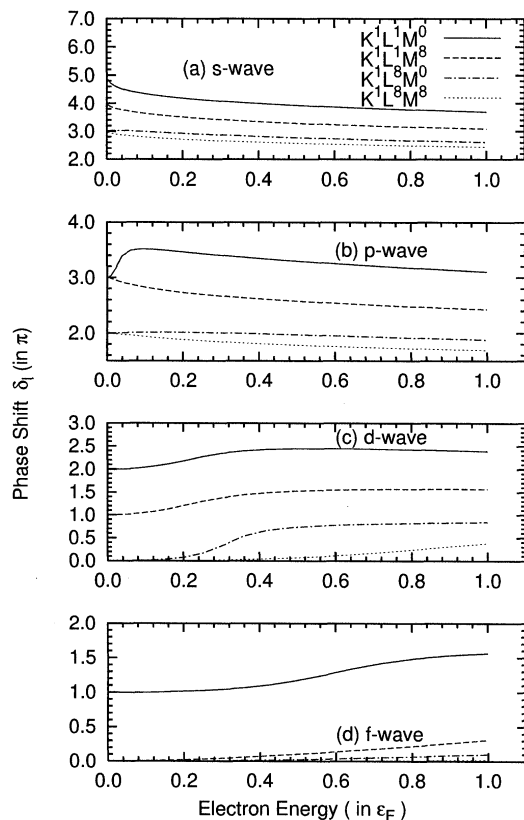


Fig. 4. Phase shifts of Ar^{q+} ions in the bulk of Al for (a) *s*, (b) *p*, (c) *d* and (d) *f* partial waves, respectively.

highly charged ions in the bulk of metallic materials by use of the LSDA/OEP-SIC method. The improvements over the existing local density functional method are: (1) we include the local spin-density functional method which allowed us to study the spin-polarized hollow atom or ion in the bulk of metallic materials; (2) we include the self-interaction correction for bound electrons, which can remove the self-interaction explicitly. Our calculated results are in reasonable agreement with the experiment.⁷

Received December 31, 2000.

Key Words

Hollow atoms; Energy structure; X-ray; Auger electron.

REFERENCES

- Burgdörfer, J. In *Review of Fundamental Processes and Applications of Atoms and Ions*; Lin, C. D., Ed.; World Scientific: Singapore, 1993; pp 517-614.
- Arnau, A. et al. *Surface Science Reports* **1997**, 27, 113.
- Winter, H.; Aumayr, F. *J. Phys. B* **1999**, 32, R39.
- Lemell, C. et al. *Phys. Rev. A* **2000**, 61, 012902.
- Limburg, J.; Das, J.; Schippers, S.; Hoekstra, R.; Morgenstern, R. *Phys. Rev. Lett.* **1994**, 73, 786.
- Limburg, J.; Schippers, S.; Hoekstra, R.; Morgenstern, R.; Kurz, H.; Aumayr, F.; Winter, H. P. *Phys. Rev. Lett.* **1995**, 75, 217.
- Briand, J. P. et al. *Phys. Rev. Lett.* **1990**, 65, 159.
- Briand, J. P.; Schneider, D.; Bardin, S.; Khemliche, H.; Jin, J.; Xie, Z.; Prior, M. *Phys. Rev. A* **1997**, 55, R2523.
- Briand, J. P. et al. *Phys. Rev. A* **1997**, 55, 3947.
- Bhalla, C. P. *Phys. Lett.* **1973**, 45A, 19.
- Karim, K. R.; Vancleave, B.; Bhalla, C. P. *J. Quant. Spectrosc. Radiat. Transfer* **1999**, 61, 227.
- Zaremba, E.; Sander, L. M.; Shore, H. B.; Rose, J. H. *J. Phys. F* **1977**, 7, 1763.
- Arnau, A.; Koohrbruck, R.; Grether, M.; Spieler, A.; Stolterfoht, N. *Phys. Rev. A* **1995**, 51, R3399.
- Parr, R. G.; Yang, W. T. *Density-Functional Theory of Atoms and Molecules*; Oxford University Press: New York, 1989.
- Chen, J.; Krieger, J.; Li, Y.; Iafrate, G. *Phys. Rev. A* **1996**, 54, 3939.
- Tong, X. M.; Chu, S. I. *Phys. Rev. A* **1997**, 55, 3406.
- Chu, S. I.; Tong, X. M.; Chu, X.; Telnov, D. *J. Chin.*

- Chem. Soc. (Tai pei)* **1999**, *46*, 361.
18. Tong, X. M.; Chu, S. I. *Phys. Rev. A* **1998**, *57*, 855.
19. Tong, X. M.; Kato, D.; Watanabe, T.; Shimizu, H.; Yamada, C.; Ohtani, S. *Phys. Rev. A* **2001**, *63*, 052505.
20. Zangwill, A. *Physics at Surface*; Cambridge University Press: Cambridge, UK, 1988.
21. Rosenberg, L.; Spruch, L. *Phys. Rev. A* **1996**, *54*, 4985.
22. Salin, A.; Arnau, A.; Echenique, P. M.; Zaremba, E. *Phys. Rev. B* **1999**, *59*, 2537.
23. Nagy, I.; Arnau, A.; Echenique, P. M. *Phys. Rev. A* **1989**, *40*, 987.
24. Zwerger, W. *Phys. Rev. Lett.* **1997**, *79*, 5270.
25. Juaristi, J. I. et al. *Phys. Rev. Lett.* **2000**, *84*, 2124.